Pramana – J. Phys. (2021) 95:18
https://doi.org/10.1007/s12043-020-02042-4

BN-Substituted non-classical fullerenes containing square rings

MARYAM ANAFCHEH[1],*, ZAHRA ABOLFATHI[1] and MANSOUR ZAHEDI[2]

[1]Department of Chemistry, Alzahra University, Vanak, Tehran 19835-389, Iran
[2]Department of Chemistry, Faculty of Sciences, Shahid Beheshti University, Evin, Tehran 19839-63113, Iran
*Corresponding author. E-mail: m.anafcheh@alzahra.ac.ir

MS received 20 October 2019; revised 6 July 2020; accepted 15 September 2020

Abstract. We performed density functional calculations to investigate the electronic and magnetic properties of BN-substituted non-classical fullerenes. The substitutional structures, binding energies, energy gaps between the highest occupied molecular orbital (HOMO) and the lowest unoccupied molecular orbital (LUMO), ionisation potentials, electron affinities, vibrational frequencies and nucleus-independent chemical shifts (NICS) were systematically investigated. The binding energies of the BN-substituted non-classical fullerenes were found to be slightly smaller than those obtained for pure non-classical fullerenes. While the reverse trend was observed for BN-substituted C_{46} and C_{32} fullerenes, it was found that the BN-substituted C_{62} fullerene has bigger ionisation potentials (IP) and smaller electron affinities (EA) than that of their parents. Because of low concentration of BN impurity, the IR spectra in the BN-substituted fullerenes are very similar to those of their parents, which can be considered as two separate regions: a low-frequency region at 200–1000 cm^{-1} corresponding to the out-of-plane bending and breathing modes and a high-frequency region at 1000–1800 cm^{-1} derived from the stretching of C–B, C–N, B–N and C–C bonds. It was shown that diatropic and paratropic ring currents of hexagons and pentagons together with the harshly antiaromatic character of the four-membered ring combine to produce a relatively small NICS at the centre of the C_{62} and C_{46} fullerene cages. The decrease in the antiaromatic and aromatic character of the B_2N_2 ring and the adjacent hexagons affects the aromaticity character of the BN-substituted fullerenes.

Keywords. Non-classical fullerene; square ring; density functional theory; nucleus-independent chemical shifts.

PACS Nos **61.48.−c; 78.30.Na; 31.15.E−**

1. Introduction

Fullerenes are generally defined as spherical polyhedral structures composed of even number of trivalent (sp^2) carbon atoms. The classic fullerenes are those polyhedrons formed by exactly 12 pentagons and $n/2-10$ hexagons (n stands for the number of carbon atoms) and follow the isolated pentagon rule (IPR), an empirical rule requiring that each pentagon in a stable fullerene should be surrounded by five hexagons [1]. Theoretical investigations demonstrate that fullerenes violating the IPR usually obey the pentagon adjacency penalty rule (PAPR) [2–4] and can only be isolated in the form of their derivatives [5,6]; this rule states that the most stable isomer bears the least number of adjacent pentagons. In fact, IPR (except for C_{72} fullerene [7]) and PAPR rules (except for C_{50} fullerene [8]) have been used as an index for predicting the structure and stability of a new fullerene [9].

On the other hand, several theoretical studies have demonstrated that non-classical fullerenes incorporating other kinds of polygons, such as square or heptagon rings, are within the range of energies spanned by the classical fullerene isomers and may be the competitors of classical fullerenes [10–22]. In 1993, Gao and Herndon [10] suggested that fullerenes with less than 60 carbon atoms might be stabilised thermodynamically by inserting square faces into them. Fowler *et al* [14] systematically designed a series of higher fullerenes with a four-membered ring and examined

Electronic supplementary material: The online version of this article (https://doi.org/10.1007/s12043-020-02042-4) contains supplementary material, which is available to authorized users.

Published online: 06 February 2021

their thermodynamic stability in some detail. Ayuela *et al* [15] and Cui *et al* [16] found that C_{62} with a heptagon is even more stable than any classical isomer. Zhao *et al* [17] found that an isomer of C_{32} with two square rings is the most stable one among all isomers built from square rings. An *et al* [18] showed that a non-classical isomer with two squares is superior to the most favourable classical isomer of fullerene C_{24}, and a cage structure incorporating a square is the lowest-energy isomer for C_{22}. Gun *et al* [19] demonstrated that the non-classical isomers of C_{54} and C_{46} with square rings are energetically unfavourable and kinetically favourable compared to their classical isomers. Overall, they have been predicted to play important roles in the growth mechanism of fullerenes [23,24]. Several non-classical fullerene-based compounds have already been available experimentally [25–27].

Substituting one or more heteroatoms (B, N, Al, P, O, S and Si) for carbon atoms through the on-ball doping results in heterofullerenes (substitutionally doped fullerenes). The first sign of substituted fullerenes, $C_{60-x}B_x$ and $C_{60-x}N_x$ ($x = 1-6$), was detected by Smalley's group [28] and Rao's group [29] in 1991, respectively. Later, the nitrogen-doped C_{60} fullerene, $C_{59}N$, was verified by Averdung *et al* [30], and its dimer, $(C_{59}N)_2$, was isolated by Pavlovich *et al* [31] in 1995.

Although, boron and nitrogen substitutions lead to electron-deficient and electron-rich systems respectively, simultaneous doping by boron and nitrogen makes the system isoelectronic to their parent fullerenes. Creating CBN fullerenes (or CBN balls) through B and N substitution is suggested to be a promising way to modify their physical, chemical and electrical properties, without seriously altering the structure of the cage. In 2003, Nakamura *et al* [32] reported the synthesis of a single BN-substituted C_{60} molecule by laser vapourisation of BC_2N graphite. Then, synthesis of BN-substituted fullerenes was reported based on different methods such as electric arc burning technique using a graphite anode which has a hole filled with boron nitride in inert atmosphere [33], high-temperature laser ablation of graphite-like BCN [34], electron-beam irradiation of various precursors [35] and substitution reaction upon irradiation with a KrF excimer laser at room temperature [36]. Theoretical investigations on single BN-substituted fullerenes such as $C_{58}BN$ indicated that heteroatoms prefer to stay together, and the structure with a BN bond on a hexagon–hexagon junction was predicted to be the most stable [37–40]. The structures and stabilities of more BN-substituted fullerenes have been theoretically studied extensively, and some rules regarding positions of heteroatoms have emerged [41–43]. For example, Pattanayak *et al* [42,43] investigated the structural patterns of successive BN substitution of 1–24 CC units of C_{60} fullerene, establishing certain rules of successive BN substitution in fullerenes, such as 'hexagonal filling rule' and 'N-site rule'. Moreover, using semiempirical AM1, MNDO and density functional theory (B3LYP/3-21G) approaches, Xu *et al* [44], Ramachandran and Sathyamurthy [45] and Ghafouri and Anafcheh [46] investigated the isomers of successive BN-substituted fullerenes $C_{50-2x}(BN)_x$ ($x = 1-15$), $C_{60-2x}(BN)_x$ ($x = 1$–24) and $C_{70-2x}(BN)_x$ ($x = 124$), respectively, in order to find out the preferred substitution patterns.

Their results also suggested that not only the number of heteroatoms but also their filling patterns may tune the properties of BN-substituted fullerenes.

Despite the relevance and a large amount of theoretical works on the BN-substituted fullerenes so far, to the best of our knowledge, a systematic study on the BN-substitution of non-classical fullerenes is still lacking in the literature. It can be a good idea to do this by theoretical calculations. So, we focus on the following important and fundamental issues: (i) Are the BN-substitution of non-classical fullerenes favourable? (ii) How does the BN-substitution affect the structure and electronic properties of non-classical fullerenes? (iii) How does the BN-substitution affect the magnetic properties and aromaticity of non-classical fullerenes? We believe that such initial investigations should provide experimentalists with a first look into the properties of these materials and will further encourage further research in this field in the future.

2. Computational method

Schlegel projections for the considered structures of non-IPR fullerenes (C_{62} and C_{46} with one square ring and C_{32} with two square rings) are depicted in figure 1. Geometries of all the systems are allowed to be fully relaxed during the density functional theory (DFT) calculations using the M06-2X functional and the 6-311G(d, p) basis set [47]. Vibrational frequency computations at the same level confirm that the 121 fully optimised structures are indeed minima. To calculate nucleus-independent chemical shift (NICS) values, ghost atoms are placed in the cage centres and individual ring centres of the considered fullerenes and BN-substituted fullerenes. All DFT calculations are performed using GAMESS suite of programs [48].

3. Results and discussion

C_{46} and C_{62} non-classical fullerenes which contain one square ring and C_{32} non-classical fullerene which

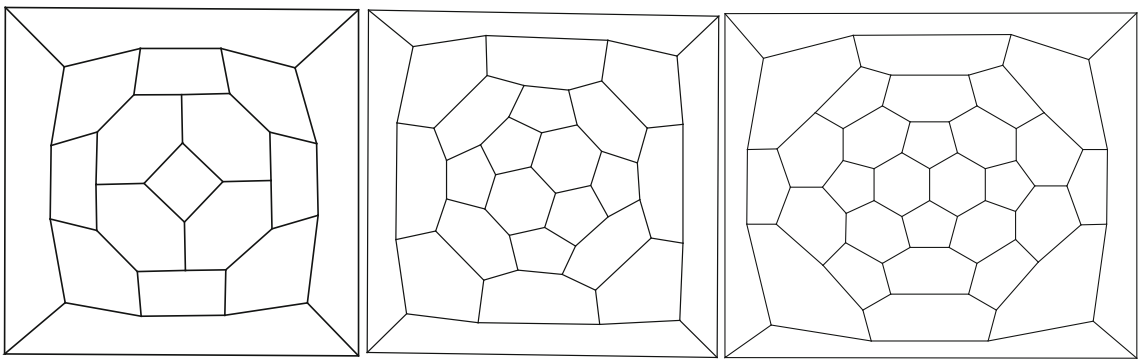

Figure 1. Schlegel diagrams of the non-IPR fullerenes, C_{62} and C_{46} with one square ring and C_{32} with two square rings.

contains two square rings are fully optimised at the M06-2X/6-311G level as the parent molecules for doping. The optimised geometries and C–C bond lengths of the considered fullerenes are shown in figure 1. Complete BN substitution of one square ring of the fullerenes will make the C_2-symmetric heterofullerenes $C_{58}B_2N_2$, $C_{42}B_2N_2$ and $C_{28}B_2N_2$. Further BN substitution of the carbon atoms is continued until complete BN substitution of one of the [4]radialene-like structures in the non-classical fullerenes happens leading to $C_{54}B_4N_4$, $C_{38}B_4N_4$ and $C_{24}B_4N_4$. The optimised structures of all the obtained heterofullerenes together with their parents are illustrated in figure 2. (Table S1 in the supplementary material lists the geometrical coordination of the considered structures). The B–N bond lengths of B_2N_2 square rings are obtained to be 1.462–1.508 Å which are in agreement with the corresponding values for boron-nitride cages reported by Napolion and Williams [49]. The C–N and C–B bond lengths of the heterofullerenes are found to be in the range of 1.356–1.460 Å and 1.455–1.555 Å, respectively.

As a stability criterion of different configurations, binding energies per atom (E_b) are calculated as follows:

$$E_b = E_M - (nE_C + mE_B + mE_N)/(n + 2m),$$

where E_M is the total energy of the heterofullerenes; n and m stand for the number of carbon and boron or nitrogen atoms, respectively. Systems with larger binding energies are known to be more stable. Binding energies of the heterofullerenes are found to be 7.77–8.36 eV/atom (listed in table 1) which are slightly smaller than those obtained for the fullerenes (8.06–8.43 eV/atom). It is noticed that BN substitution of larger non-classical fullerenes is more favourable than smaller cages.

Previous theoretical studies pointed out that the doping of fullerenes affects their electronic structures by modifying the highest occupied molecular orbital (HOMO) and lowest occupied molecular orbital (LUMO) energies. In this study, the IP and EA values for the considered models are computed to examine their electron-accepting and electron-donating abilities, which is followed by adding/removing one electron to the neutral molecule and evaluating the energy difference using the equations IP $= E_{M^{+1}} - E_M$ and EA $= E_M - E_{M^{-1}}$ to accomplish the first IP and EA, respectively. The energies of ionic states ($E(M^{+1})$ and $E(M^{-1})$) are also calculated at the M06-2X/6-311G level of theory by removing/adding one electron to/from the neutral form of each molecule, using the optimised geometry of the neutral form. The IP, EA and HOMO–LUMO energy gaps (E_g) for the BN-substituted non-classical fullerenes are summarised in table 1.

As seen, the BN-substituted C_{62} fullerenes have larger IP and smaller EA than their parent, suggesting that the considered BN-substituted C_{62} fullerenes lose electrons with somewhat more difficulty to form positive ions and also obtain electrons with more difficulty to form anions. In other words, it is more difficult to oxidise or reduce the BN-substituted C_{62} fullerenes than their corresponding pristine C_{62} fullerene. The reverse trend is observed for the BN-substituted C_{46} and C_{32} fullerenes, having smaller IPs and bigger EAs than their pure carbon cages. The HOMO–LUMO energy gaps for the non-classical fullerenes C_{62}, C_{46} and C_{32} are obtained to be 2.19, 2.37 and 3.56 eV, respectively. In comparison with their parents, HOMO–LUMO gap increases to 2.58 eV for $C_{58}B_2N_2$ while it decreases to 1.84 and 2.49 eV for $C_{42}B_2N_2$ and $C_{28}B_2N_2$, respectively. The same increasing or decreasing trend is observed for HOMO–LUMO gaps of the C_{62}, C_{46} and C_{32} fullerenes with a completely BN-substituted [4]radialene-like structure, 2.47,

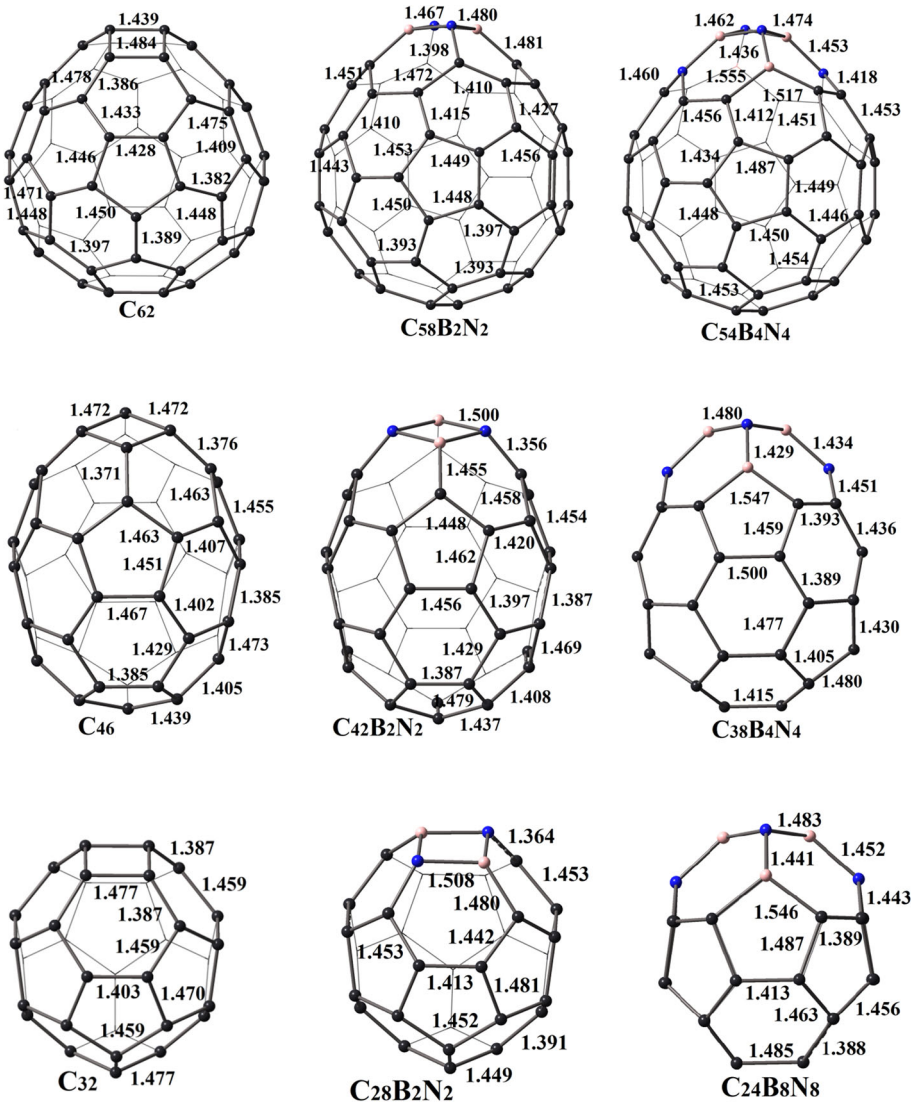

Figure 2. The optimised geometries of the BN-substituted non-IPR fullerenes together with their parents. The geometrical parameters (in Å) are shown.

Table 1. Total energies (E_t in a.u.), HOMO–LUMO energy gaps (E_g, eV), IP (in eV) and EA (in eV) for the BN-substituted non-classical fullerenes and their parents.

	E_t	E_{bin}	E_g	IP	EA
C_{62}	−2360.10327	8.43	2.19	5.91	3.72
$C_{58}B_2N_2$	−2367.07864	8.36	2.58	6.03	3.45
$C_{54}B_4N_4$	−2374.01117	8.27	2.47	6.06	3.58
C_{46}	−1750.78270	8.27	2.37	6.43	4.06
$C_{42}B_2N_2$	−1757.71937	8.16	1.84	5.98	4.14
$C_{38}B_4N_4$	−1764.70704	8.07	2.29	6.37	4.08
C_{32}	−1217.68082	8.06	3.56	6.83	3.26
$C_{28}B_2N_2$	−1224.62986	7.90	2.49	6.37	3.88
$C_{24}B_4N_4$	−1231.60422	7.77	3.19	6.62	3.43

2.29 and 3.19 eV for $C_{54}B_4N_4$, $C_{38}B_4N_4$ and $C_{24}B_4N_4$ heterofullerenes, respectively.

The calculated infrared spectra of non-classical fullerenes are shown in figure 3. The whole spectra (200–1700 cm^{-1}) related to the fullerenes can be considered in two regions. The first region is in the range of 200–1000 cm^{-1}, in which the vibrational modes correspond to the out-of-plane bending and breathing modes. In this region, the peaks seen at 200–600 cm^{-1} with very low intensity are related to the out-of-plane bending of the C–C–C angles of the square ring, leading to breathing movement or a cradle-like displacement for square rings. The frequencies from 600 to 800 cm^{-1} with medium or low intensity are assigned to the out-of-plane bending of C–C–C angles of hexagon and pentagon rings, leading to breathing modes of fullerene cages. The second region is in the range of 1000–1800 cm^{-1}; most spectra show their highest peak at 1400–1500 cm^{-1}, which is assigned to the stretching of the C−C bonds.

The IR spectra simulated for the BN-substituted non-classical fullerenes are very similar to those of their parent fullerenes because of low concentration of B–N impurity, separated into two regions: a low-frequency region at 200–1000 cm^{-1} and a high-frequency region at 1000–1700 cm^{-1}. BN doping leads to the decrease of υ_{min} for heterofullerenes, see figure 4. The stronger absorptions at 1400–1700 cm^{-1} are derived from the stretching of C–B, C–N, B–N and C–C bonds, while the weaker absorptions at 700–850 cm^{-1} correspond to the out-of-plane bending and breathing modes.

Aromaticity is commonly explained by the ring current theory that attributes the unique properties shared by aromatic molecules to form a special electron delocalisation. The geometry of a conjugate molecule allows the electrons to move along a cyclic path for delocalisation. The NICS, which has been proposed by Schleyer and co-workers in 1996 [50,51], is a simple and efficient aromaticity probe. NICS can be computed easily at the cage centres of fullerenes and their derivatives, using modern quantum chemical methods [52,53]. NICS values obtained at the centres of the cages and of the individual ring provide appropriate insights of the electron delocalisation, molecular aromaticity and molecular magnetic properties. So, to evaluate the effect of dopants on the mobility of electrons and aromaticity properties of the cages, NICS values are calculated at the centres of the cages and the individual rings of the onsidered fullerene cages. The calculated NICSs for the BN-substituted non-classical fullerenes and their parents are shown in figure 4. According to the definition of NICS, the more negative NICS values in the interior positions of the rings or the cages indicate the presence of stronger aromaticity. The NICS value at the cage centre of C_{62} is calculated to be −7.00 ppm which is close to that reported for C_{60} [54]. C_{62} is found to contain diatropic hexagons and paratropic pentagons with NICS values in the range of (−6.3)–(−5.6) and (+2.9)–(+4.7) ppm at the ring centres, respectively. The corresponding ring currents together with the antiaromatic character of the four-membered ring (30.5 ppm) combine to produce a relatively negative NICS (−7.00 ppm) at the centre of the C_{62} cage. A decrease in the antiaromatic character of the four-membered ring in C_{46} together with the decrease in the number of the diatropic hexagonal rings leads to the NICS value (−8.2 ppm) in this cage. The very high aromaticity of the C_{32} cage (−35.3 ppm) is very similar to the classical C_{36} fullerene, in both of which hexagons are locally more aromatic than pentagons [55].

While the BN-substituted $C_{58}(BN)_2$ is slightly more aromatic than C_{62} with a NICS value of −8.5 ppm, NICS value of $C_{54}(BN)_4$ is obtained to be −6.8 ppm. At first sight, this finding is counterintuitive, as the electrons in the BN unit are mainly localised on nitrogen as the lone pair. This issue can be resolved by considering the aromaticity at the centres of the individual rings. As seen, antiaromatic and aromatic characters of the B_2N_2 ring and the adjacent hexagons decrease in $C_{58}(BN)_2$ and $C_{54}(BN)_4$, respectively, while the NICS values of the other five- and six-membered rings are slightly affected by BN doping. The compensation between diatropic and paratropic ring currents yields a more negative NICS value in $C_{58}(BN)_2$ than in C_{62} itself. Similar ring currents combine to produce non-aromatic character at the centre of the BN-substituted C_{46} fullerene. It is worthwhile to note that BN doping affects aromaticity of the whole rings in C_{32}, and leads to a decrease in the aromatic character of $C_{28}(BN)_2$ and $C_{24}(BN)_4$ in comparison with their parent.

4. Conclusion

The BN substitution of non-classical fullerenes is investigated in terms of geometry, energies, electronic structures, IPs, EAs, vibrational frequencies and NICS based on DST. According to the obtained results, we emphasise the following points: (1) the binding energies of BN-substituted non-classical fullerenes are slightly smaller than those obtained for pure non-classical fullerenes, (2) unlike BN-substituted C_{62} fullerene, BN-substituted C_{46} and C_{32} fullerenes have smaller IPs and larger EAs. A similar trend is observed for H–L gaps, (3) the IR spectrum simulated for the BN-substituted heterofullerenes and their parents can be considered in two regions: the energy modes at low-frequency correspond to out-of-plane bending and breathing modes and high-frequency

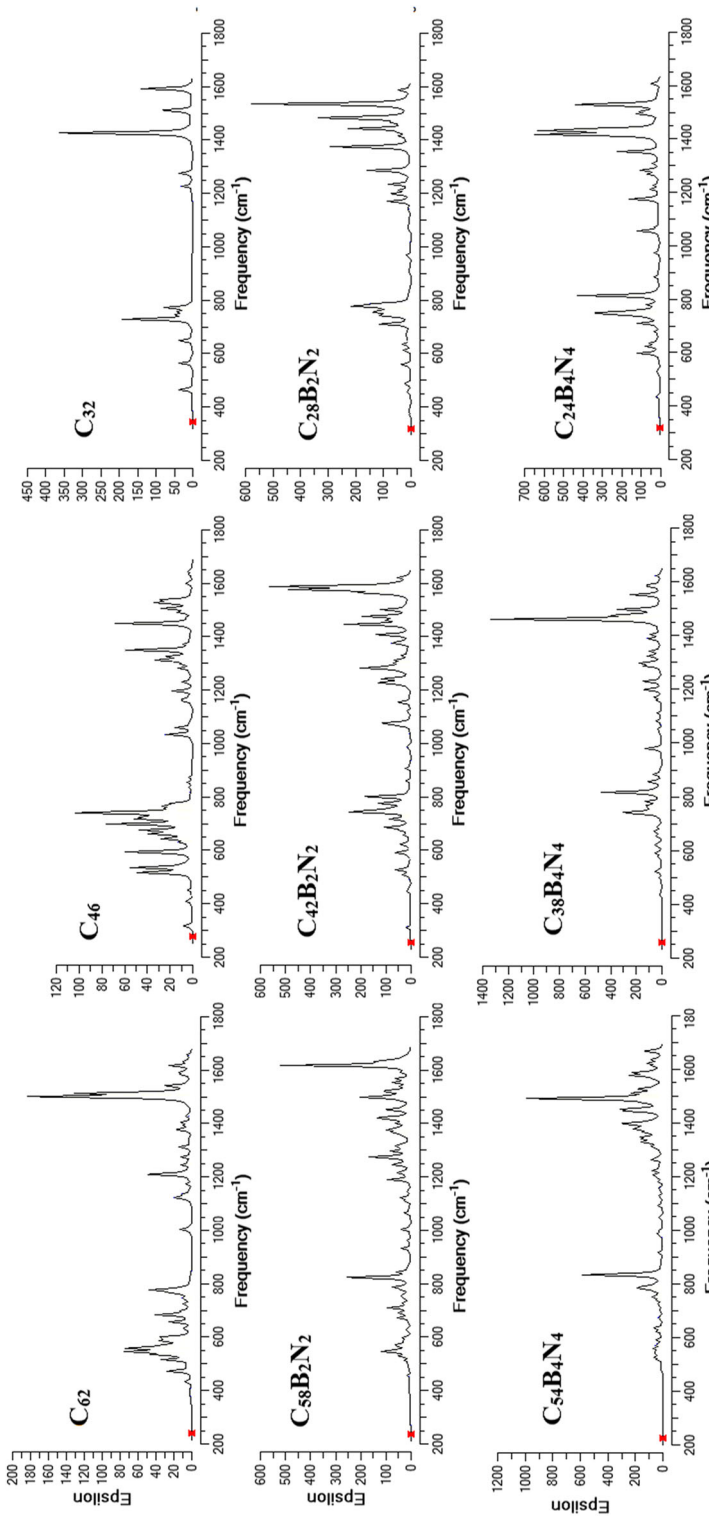

Figure 3. The calculated infrared spectra of the BN-substituted non-classical fullerenes together with their parents.

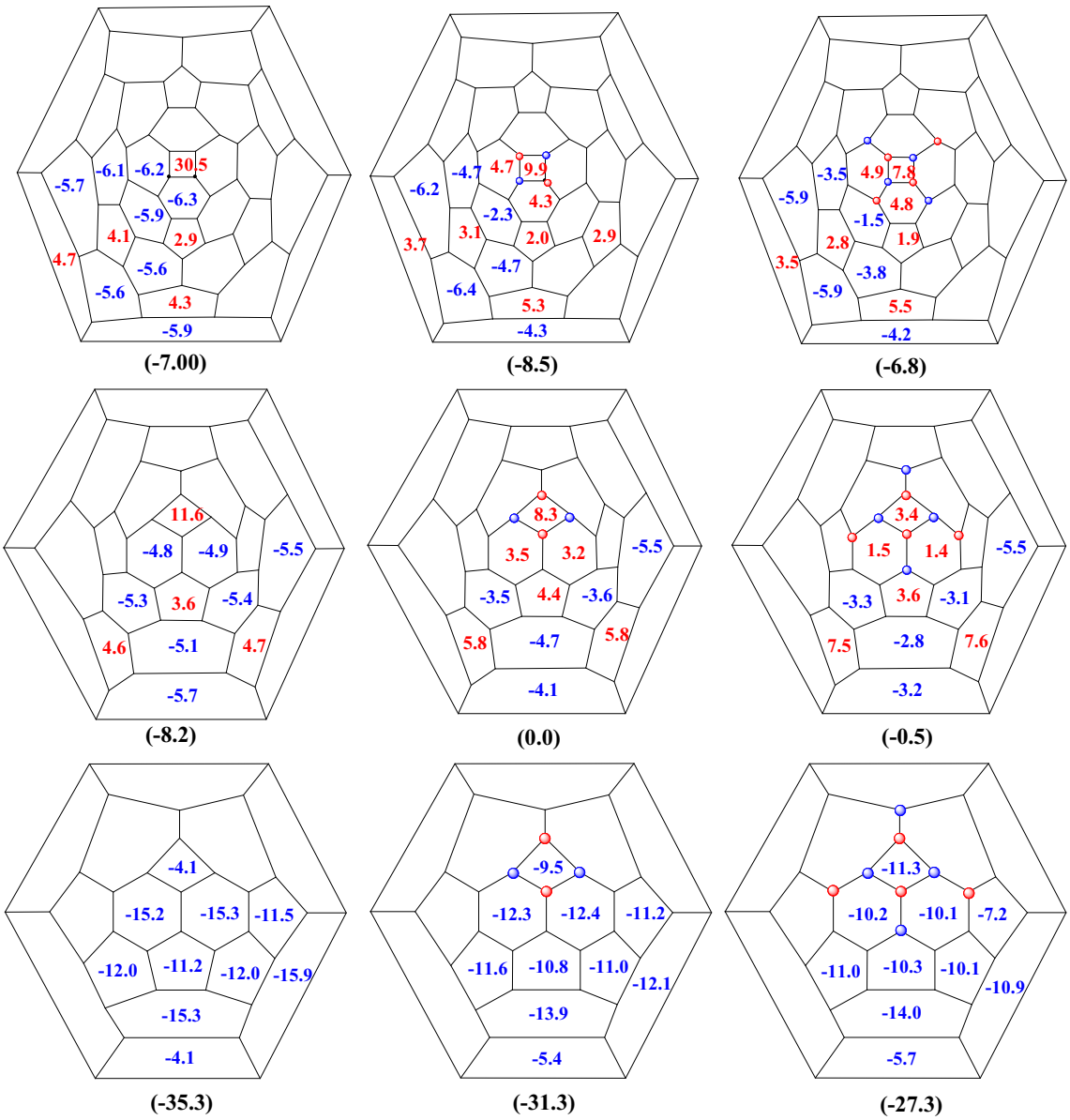

Figure 4. 2D projections of the considered structures of the BN-substituted non-classical fullerenes together with their parents. Computed nucleus-independent chemical shifts (NICS) calculated at the centres of the cages and of the individual rings are shown. Small filled red and blue circles represent boron and nitrogen atoms, respectively.

in the region is assigned to stretching of the C–B, C–N, B–N and C–C bonds, (4) the compensation between diatropic and paratropic ring currents of the hexagons and pentagons of C_{62} and C_{42} together with the antiaromatic character of the four-membered ring yields relatively small NICS value at the centre of these cages, (5) the C_{32} fullerene with two square rings has high aromatic character. Similar to the classical C_{36} fullerene, hexagons of C_{32} are locally more aromatic than pentagons. Finally, decrease of the antiaromatic and aromatic characters of the B_2N_2 ring and the adjacent hexagons, respectively, affects NICS value and aromaticity at the cage centre of the BN-substituted fullerenes.

Acknowledgements

The authors gratefully acknowledge the financial support from the Research Council of Alzahra University.

References

[1] H W Kroto, *Nature* **329**, 529 (1987)
[2] E E B Campbell, P W Fowler, D Mitchell and F Zerbetto, *Chem. Phys. Lett.* **250**, 544 (1996)
[3] E Albertazzi, C Domene, P W Fowler, T Heine, G Seifert, C Van Alsenoy and F Zerbetto, *Phys. Chem. Chem. Phys.* **1**, 2913 (1999)

[4] S Diaz-Tendero, F Martin and M Alcami, *Chem. Phys. Chem.* **6**, 92 (2005)
[5] K Ziegler, A Mueller, K Y Amsharov and M Jansen, *J. Am. Chem. Soc.* **132**, 17099 (2010)
[6] Y-Z Tan, T Zhou, J Bao, G-J Shan, S Y Xie, R-B Huang and L-S Zheng, *J. Am. Chem. Soc.* **132**, 17102 (2010)
[7] Z Slanina, K Ishimura, K Kobayashi and S Nagase, *Chem. Phys. Lett.* **384**, 114 (2004)
[8] S Díaz-Tendero, M Alcamí and F Martín, *Chem. Phys. Lett.* **407**, 153 (2005)
[9] A R Khamatgalimov and V I Kovalenko, *Russ. Chem. Rev.* **85**, 836 (2016)
[10] Y D Gao and W C Herndon, *J. Am. Chem. Soc.* **115**, 8459 (1993)
[11] B I Dunlap and R Taylor, *J. Phys. Chem.* **98**, 11018 (1994)
[12] D Babić and N Trinajstić, *Chem. Phys. Lett.* **23**, 239 (1995)
[13] P W Fowler, T Heine, D Mitchell, G Orlandi, R Schmidt, G Seifert and F Zerbetto, *J. Chem. Soc. Faraday Trans.* **92**, 2203 (1996)
[14] P W Fowler, T Heine, D E Manolopoulos, D Mitchell, G Orlandi, R Schmidt, G Seifert and F Zerbetto, *J. Phys. Chem.* **100**, 6984 (1996)
[15] A Ayuela, P W Fowler, D Mitchell, R Schmidt, G Seifert and F Zerbetto, *J. Phys. Chem.* **100**, 15634 (1996)
[16] Y H Cui, D L Chen, W Q Tian and J K Feng, *J. Phys. Chem. A* **111**, 7933 (2007)
[17] X Zhao, Z Slanina, M Ozawa, E Osawa, P Deota and K Tanabe, *Fullerene Sci. Technol.* **8**, 595 (2000)
[18] W An, N Shao, S Bulusu and X C Zeng, *J. Chem. Phys.* **128**, 084301 (2008)
[19] L-H Gan, J-Q Zhao and F Pan, *J. Mol. Struct. Theochem.* **953**, 24 (2010)
[20] J Aihara, *J. Chem. Soc. Faraday Trans*. **91**, 4349 (1995)
[21] J An, L H Gan, X Fan and F Pan, *Chem. Phys. Lett.* **511**, 351 (2011)
[22] J Aihara, *Internet Electron. J. Mol. Des.* **2**, 492 (2003)
[23] R L Murry, D L Strout, G K Odom and G E Scuseria, *Nature* **366**, 665 (1993)
[24] E Hernandez, P Ordejon and H Terrones, *Phys. Rev. B* **63**, 193403 (2001)
[25] W Qian, S-C Chuang, R B Amador, T Jarrosson, M Sander, S Pieniazek, S I Khan and Y Rubin, *J. Am. Chem. Soc.* **125**, 2066 (2003)
[26] P A Troshin, A G Avent, A D Darwish, N Martsinovich, A K Abdul-Sada, J M Street and R Taylor, *Science* **309**, 278 (2005)
[27] I N Ioffe, C B Chen, S F Yang, L N Sidorov, E Kemnitz and S I Troyanov, *Angew. Chem. Int. Edit.* **49**, 1 (2010)
[28] T Guo, C Jin and R E Smalley, *J. Phys. Chem.* **95**, 4948 (1991)
[29] T Pradeep, V Vijayakrishnan, A K Santra and C N R Rao, *J. Phys. Chem.* **95**, 10564 (1991)
[30] J Averdung, H Luftmann, I Schlachter and J Mattay, *Tetrahedron* **51**, 6977 (1995)
[31] J Pavlovich, R Gonzalez, J C Hummelen, B Knight and F Wudl, *Science* **269**, 1554 (1995)
[32] T Nakamura, K Ishikawa, A Goto, M Ishihara, T Ohara and Y Koga, *Diamond Relat. Mater.* **12**, 1908 (2003)
[33] J Piechota, P Byzsewski, R Jablonski and K Antonova, *Fullerene Sci. Technol.* **4**, 491 (1996)
[34] T Nakamura, K Ishikawa, K Yamamoto, T Ohana, S Fujiwara and Y Koga, *Phys. Chem. Chem. Phys.* **1**, 2631 (1999)
[35] D Golberg, Y Bando, O Stephan, L Bourgeois, K Kurashima, T Sasaki, T Sato and C Goringe, *J. Electron. Microsc.* **48**, 701 (1999)
[36] T Nakamura, K Ishikawa, A Goto, M Ishihara, T Ohana and Y Koga, *Diamond Relat. Mater.* **10**, 1228 (2001)
[37] T Kar, J Pattanayak and S Scheiner, *J. Phys. Chem. A* **107**, 8630 (2003)
[38] F Liu, L Meng and S Zheng, *J. Phys. Chem. B* **110**, 6666 (2006)
[39] Z Chen, K Ma, L Chen, H Zhao, Y Pan, X Xao, A Tang and J Feng, *J. Mol. Struct.: Theochem.* **452**, 219 (1998)
[40] K Esfarjani, K Ohno and Y Kawazoe, *Phys. Rev. B* **50**, 17830 (1994)
[41] S H Xu, M Y Zhang, Y Zhao, B G Chen, J Zhang and C C Sun, *Chem. Phys. Lett.* **418**, 297 (2006)
[42] J Pattanayak, T Kar and S Scheiner, *J. Phys. Chem. A* **105**, 8376 (2001)
[43] J Pattanayak, T Kar and S Scheiner, *J. Phys. Chem. A* **106**, 2970 (2002)
[44] X Xu, Z Shang, G Wang, R Li, Z Cai and X Zhao, *J. Phys. Chem. A* **109**, 3754 (2005)
[45] C N Ramachandran and N Sathyamurthy, *J. Phys. Chem. A* **111**, 6901 (2007)
[46] R Ghafouri and M Anafcheh, *J. Phys. Chem. Solids* **73**, 1378 (2012)
[47] Y Zhao and D G Truhlar, *Theor. Chem. Account.* **120**, 215 (2008)
[48] M W Schmidt, K K Baldridge, J A Boatz, S T Elbert, M S Gordon, J H Jensen, S Koseki, N Matsunaga, K A Nguyen, S J Su, T L Windus, M Dupuis and J A Montgomery, *J. Comput. Chem.* **14**, 1347 (1993)
[49] B Napolion and Q L Williams, *Chem. Phys. Lett.* **490**, 210 (2010)
[50] P V R Schleyer, C Maerker, A Dransfeld, H Jiao and N J R V E Hommes, *J. Am. Chem. Soc.* **118**, 6317 (1996)
[51] Z Chen, C S Wannere, C Corminboeuf, R Puchta and P V R Schleyer, *Chem. Rev.* **105**, 3842 (2005)
[52] X Lu and Z Chen, *Chem. Rev.* **105**, 3643 (2005)
[53] M Bühl and A Hirsch, *Chem. Rev.* **101**, 1153 (2001)
[54] Z Chen, H Jiao, A Hirsch and W Thiel, *J. Org. Chem.* **66**, 3380 (2001)
[55] Z Chen, H Jiao, M Buhl, A Hirsch and W Thiel, *Theor. Chem. Acc.* **106**, 352 (2001)